

Exponential relaxation of optical emissions in sprites

Christopher P. Barrington-Leigh

Space Sciences Laboratory, University of California, Berkeley, Berkeley, California, USA

Victor P. Pasko

Communications and Space Sciences Laboratory, Pennsylvania State University, University Park, Pennsylvania, USA

Umran S. Inan

Space, Telecommunications, and Radioscience Laboratory, Stanford University, Stanford, California, USA

Received 27 March 2001; revised 9 July 2001; accepted 14 July 2001; published 31 May 2002

[1] The optical emissions in a large number of bright sprites observed over one storm in 1998 exhibit a relaxation that is closely exponential in time. This feature was unexpected but might be explained by the presence of quasi-constant electric fields over times of several milliseconds, in which case the optical relaxation would be a direct indication of the exponentially changing electron density. The relaxation rates for sprites appear to have an upper bound that is consistent with the dissociative electron attachment rates expected at sprite altitudes. The experimental results are consistent with existing large-scale electrodynamic models of sprites as well as with the streamer mechanism as the underlying physical process for sprite ionization. *INDEX TERMS:* 2423 Ionosphere: Ionization mechanisms; 2427 Ionosphere: Ionosphere/atmosphere interactions (0335); 3324 Meteorology and Atmospheric Dynamics: Lightning; 3332 Meteorology and Atmospheric Dynamics: Mesospheric dynamics; *KEYWORDS:* Sprite, streamer, photometry, exponential relaxation, electron density, ion density

1. Introduction

[2] A photometric array named the Fly's Eye was previously used to detect a predicted signature of "elves," the lower ionospheric (80–95 km altitude) optical flash due to heating by an impinging electromagnetic pulse launched by intense lightning currents [Inan *et al.*, 1997; Barrington-Leigh and Inan, 1999; Barrington-Leigh *et al.*, 2001]. Nine narrow individual photometer fields-of-view of ($2.2^\circ \times 1.1^\circ$) are horizontally arrayed to provide a spatial resolution of ~ 20 km at a range of 500 km. The Fly's Eye array, operated with a high-speed triggered data acquisition system, bore-sighted image-intensified CCD video camera, and a VLF radio receiver, was also used to investigate sprites [Barrington-Leigh *et al.*, 1999, 2001]. Sprites are diffuse to highly structured discharges lasting 5–100 ms and extending from 40 to 85 km altitude which result from intense electric fields following a major redistribution of electric charge in the troposphere, usually in association with a positive cloud-to-ground return stroke. Sprites may involve or consist of a brief diffuse luminous region above ~ 70 km altitude [Pasko *et al.*, 1998a] named the sprite "halo" [Barrington-Leigh *et al.*, 2001] but typically include columnar or filamentary optical structures thought to correspond to the propagation path of corona streamers [Pasko *et al.*, 1998a; Stanley *et al.*, 1999].

[3] Several criteria used for the identification of elves in narrow field-of-view photometers are described by Barrington-Leigh and Inan [1999]. One additional criterion not mentioned there is the fast relaxation timescale (<100 μ s) which is often a characteristic of optical pulses due to elves. Such fast relaxation, observed in narrow field of view photometers, is not typical for scattered light from lightning [Thomason and Krider, 1982; Guo and Krider, 1982], and observations outlined below show that it is also generally not observed for sprites.

[4] On the night of 19 July 1998, a large mesoscale convective system over northwestern Mexico produced exceptionally bright sprites. Measurements were made from the Langmuir Laboratory for Atmospheric Research ($107.19^\circ\text{W} \times 33.98^\circ\text{N} \times 3200$ m) in New Mexico using the Fly's Eye camera, optical array, and VLF receiver. In addition, many sprites were bright enough to be visible to the unaided and unadapted eye.

[5] Determination of total sprite luminous lifetimes has generally been challenging [Raider and Mende, 1995; Winckler *et al.*, 1996]. Video recordings give generally poor (>1 ms) time resolution and some systems, such as the image intensifier of the Fly's Eye video, exhibit a phosphor persistence following intensely bright signals. This afterglow may last for several frames, making our instrument unreliable for quantifying long sprite durations. However, photometers designed with high time resolution exhibit no such "ghosting" but, because they rely on the photoelectric effect, are not optimized for measurement in the near infrared region of the spectrum (as compared with band-gap materials) [Winckler *et al.*, 1996]. Moreover, because a photometer field of view is typically large compared with an imager pixel or with variation in sprite structure, the spatially integrated background can make difficult the task of measuring slowly varying, weak signals. In the Fly's Eye photometers, the slow glow of typical sprites often appears to decay gradually into the background photometer signal level, implying the existence of even more persistent, unresolved luminosity. Extra bright sprites facilitate the measurement of these longer timescales using the Fly's Eye.

[6] Sprites are known sometimes to occur well after (up to tens of milliseconds) an associated lightning return stroke [Bell *et al.*, 1998]. It has been proposed that this property may be due to slowly varying currents, possibly undetectable by remote ELF radio measurements, which may be flowing along the ionized return stroke channel or possibly horizontally within the thundercloud [Bell *et al.*, 1998; Cummer *et al.*, 1998; Cummer and Stanley, 1999; Johnson and Inan, 2000]. In some cases, a series of (positive) cloud-to-ground discharges may occur sequentially

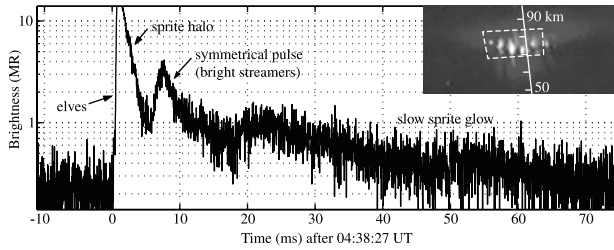


Figure 1. Photometric features of a bright sprite. The signal from one narrow field-of-view photometer is shown for part of an event at 0438:27 UT on 19 July 1998. This sprite occurred 0.5 s after a series of intense sprites associated with a series of positive cloud-to-ground lightning discharges. The inset shows a video field of the sprite from the Fly's Eye camera, superposed by a box showing the approximate field-of-view of the photometer and a scale showing altitudes overlying a causative CG.

over a large horizontal distance within a fraction of a second (spider lightning), suggesting the existence of an expansive traveling network of intracloud currents [Lyons, 1996]. These events are typically accompanied by a series of sprites mirroring the propagation of the lightning below (“dancing sprites”). In such cases several sprites can occur with continuous luminosity over a large fraction of a second and may appear to be associated with several lightning strokes. This paradigm was typical for the sprites observed on 19 July 1998.

[7] In the following sections, several notable features of sprites are discussed in the context of the observations carried out on 19 July 1998. The extra signal available on this night may have highlighted some hard-to-observe (with instrumentation used so far) but common features of sprites, or the observations, may correspond only to the special case of unusually intense ionization and emissions. Several multicolor photometry and imaging studies have suggested that the degree of ionization in sprites can vary greatly [Armstrong *et al.*, 1998b, 2000] and that brighter sprites do not necessarily exhibit a higher fraction of emissions from ionized states [Heavner *et al.*, 1998].

2. Timescales in Sprites Photometry

[8] Figure 1 shows a sample photometric record of a bright sprite cluster and illustrates the existence of more than one timescale in sprites. The inset image shows an intense sprite halo [Barrington-Leigh *et al.*, 2001; Wescott *et al.*, 2001] and bright patches near its lower boundary at \sim 75 km, which appear to have initiated downward streamers in a manner similar to that described by Stanley *et al.* [1999]. This event is accompanied by the photometric signature of elves [Inan *et al.*, 1997] in the full array of photometers (not shown). The record from a single narrow field-of-view photometer shows an optical pulse, initially owing to elves, which becomes very bright and is protracted for >2 ms. This brightness is likely to be due to the sprite halo evident in the video image. Approximately 6 ms after the event onset a pulse with characteristic rise and fall times both of \sim 2 ms appears and then relaxes into >50 ms of less intense glow.

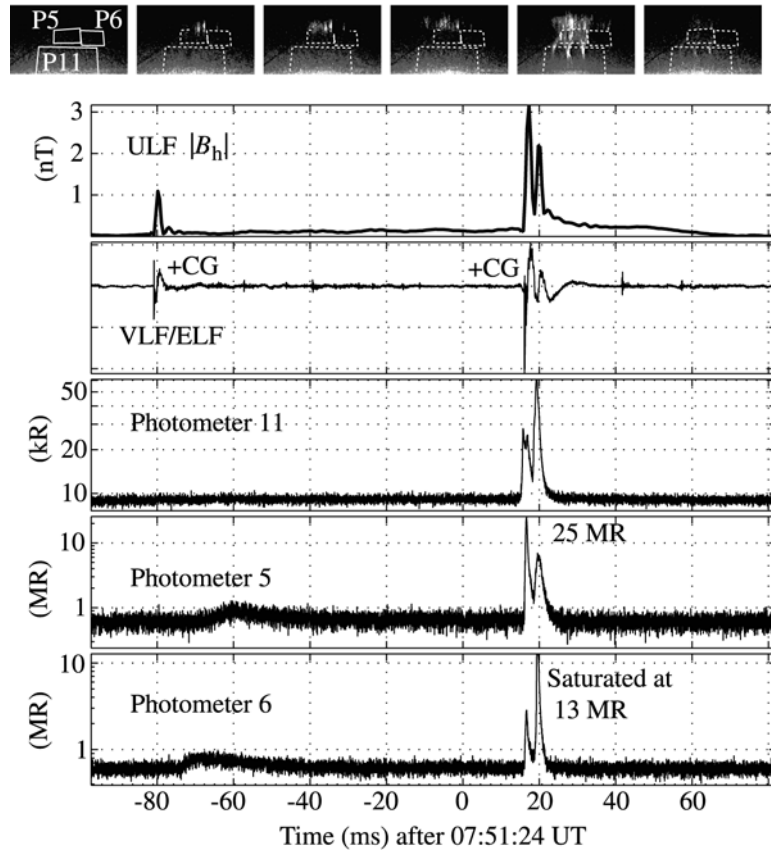


Figure 2. Slow sprite development and ULF currents on 6 August 1998. The ULF magnetic field is obtained by integrating in time data (provided by Martin Füllekrug) from a magnetic loop receiver. Photometers 5 and 6 have narrow ($2.2^\circ \times 1.1^\circ$) field-of-views, while the dimensions of Photometer 11 are 3 times as large. The video images are shown time-aligned to the plots. According to NLDN, the two lightning discharges were 31 km apart.

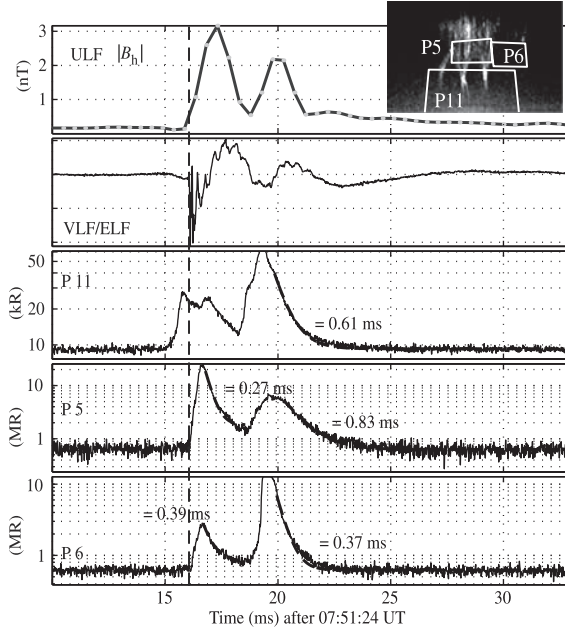


Figure 3. Sprite preceding cloud-to-ground lightning. A close-up of Figure 2.

[9] This example highlights several features of sprites which were frequently observed on 19 July 1998 and in the course of the annual sprite campaigns conducted by the authors. Many events exhibit a bright peak which is often only a few milliseconds in duration and tends to grow and decay with similar timescales. In addition, overall photometric durations much larger than 10 ms were found to be normal on this day, in contrast to the observations of Winckler *et al.* [1996].

[10] Cummer and Stanley [1999] found that the peak in optical intensity of sprites occurred after the propagation of streamers to their lowest altitudes was complete. The same phenomenology is observed for the halo event detailed by Barrington-Leigh *et al.* [2001] and may be analogous to the luminous return stroke of lightning following the connection of a leader channel to ground. In this analogy, the slower sprite glow evident in Figure 1 may correspond to lesser excitation of the channel during the analogue of the continuing current phase in lightning.

[11] Measurements from the Fly's Eye's video camera, ELF/VLF sferic receiver, and three photometers, as well as from an ultra low frequency (ULF, < 30 Hz) search coil (operated by Universität Frankfurt), are shown in Figures 2 and 3.

[12] Several notable features are apparent in the event shown in Figure 2. Two cloud-to-ground discharges cause sprites exhibiting both short, bright features and a longer dimmer luminosity which is not well resolved by the photometers. On the basis of the video images, it is likely that this sprite sustained some luminosity during the entire time between the two lightning strokes. The ULF magnetic field persists at a low level during the interval between the lightning strokes (compared with the magnetic field magnitude before the first stroke), indicating the existence of a vertical current flowing continuously for >140 ms after the first stroke. Figure 3 shows the unusual fact that the brightening of the sprite in photometer 11 appears to anticipate the onset of the second cloud-to-ground discharge. Given the 31 km proximity of the two lightning strokes as reported by the National Lightning Detection Network (NLDN), it is likely that they were closely coupled electrically through intracloud currents. The timescale for stepped leader breakdown is >10 ms altogether, and ~1 ms for the final leader pulse preceding the return stroke [Uman, 1987, pp. 14–16], implying that the channel taken by the second return stroke in

Figure 2 must have been developing well before the onset of the bright optical signature. While recent results of Cummer and Füllekrug [2001] suggest that inferred vertical current moments may be sufficient to account for sprite breakdown even in long-delayed (>30 ms) sprites, the occurrence of a sprite just preceding the return stroke in Figure 3 suggests that a large (horizontal) charge motion within the cloud may have both led to a sprite and been involved in the initiation of the return stroke, which would indicate that horizontal currents might themselves sometimes excite sprites.

[13] For reasons discussed elsewhere [Cummer *et al.*, 1998; Johnson and Inan, 2000], it is difficult to determine experimentally the relative contributions of vertical and horizontal lightning currents in the production of mesospheric electric fields. Discussion of sustained lightning source currents throughout the rest of this paper could in principle apply to intracloud charge redistribution or to cloud-to-ground currents.

3. Observations of Exponential Photometric Decay

[14] While the relative timing of the sprite and lightning in Figure 3 is highly unusual, another remarkable feature of this event is one that was commonly observed in photometry of bright sprites on this day. The dashed lines superposed on the photometer traces in Figure 3 show curves of the form

$$y(t) = C + Ae^{-t/\tau_o} \quad (1)$$

fit to the data by choosing values of C , A , and τ_o . The decay of bright optical pulses due to sprites is found in a large number of cases to closely follow the exponential form in (1) over several time constants τ_o , although the value of τ_o varies considerably between different optical peaks. This rather remarkable feature of sprite optical decay has only been mentioned for one case [Suszczynsky *et al.*, 1998] but may be discernable in photometric data of Winckler *et al.* [1996] and Fukunishi *et al.* [1996].

[15] An electric field imposed on a uniform, weakly conductive medium by a rapid rearrangement of charges is expected to decay exponentially in time [Pasko *et al.*, 1997, 1999]. Indeed, the typical timescales τ_o for the observed decay are comparable to the expected ambient electric relaxation time constant $\tau_E = \epsilon_0/\sigma$ at the observed altitudes (Figure 4). Here ϵ_0 is the permittivity of free space, and σ is the local conductivity. However, the optical emissions should not relax exponentially in such a case because of their highly nonlinear dependence on the electric field strength. Figure 5 shows this electric field dependence of the excitation rates v_k responsible for the dominant optical emissions in sprites. The electric fields shown are normalized to the local conventional breakdown field E_k , which is proportional to the local air density. Also shown are the coefficients of ionization (v_i) and electron dissociative attachment (v_a), defined such that the electron density follows

$$\frac{dn_e}{dt} = [v_i(E) - v_a(E)]n_e. \quad (2)$$

The optical emissions (i.e., number of photons emitted per unit time from unit volume) due to excited state k are then [e.g., Pasko *et al.*, 1997]

$$A_k n_k \simeq v_k(E)n_e, \quad (3)$$

where n_k is the density of the excited state and A_k is the radiation transition rate. This expression neglects the effect of quenching, which is negligible above 50 km for the dominant optical bands in sprites, and the effect of cascading, which does not affect the arguments that follow. The approximation in (3) is valid because the radiative decay times for the relevant states are fast (<6 μ s) in

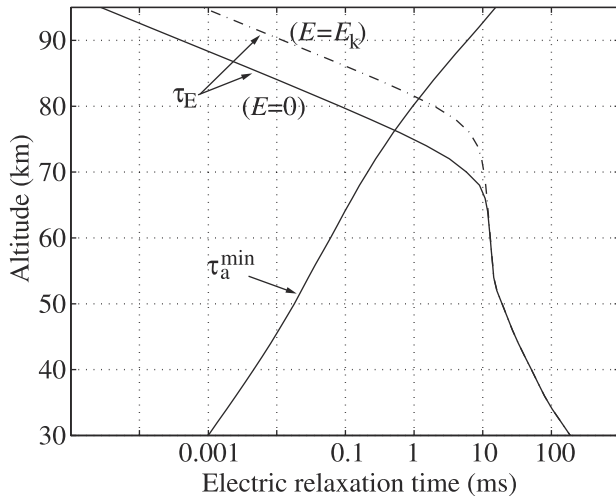


Figure 4. Electric relaxation and attachment timescales as a function of altitude. τ_a^{\min} corresponds to the two-body dissociative attachment rate at $E \simeq 0.8 E_k$; see Figure 5. Values of $\tau_E = \epsilon_0/\sigma$ are calculated using an ambient nighttime electron density.

comparison with any changes in the electron density. Thus, considering the form of v_k shown in Figure 5, it may be seen that the optical emission rate does not vary in a simple way in an electric field which is relaxing exponentially with time.

[16] However, the observed photometric exponential relaxation would be obtained if we adopt the ad hoc assumption that the electric field remains approximately constant in time during the lifetime of the sprite. For $E = E_0 = \text{constant}$, $A_k n_k \simeq v_k(E_0) n_e(t)$ and we have from (2),

$$n_e = n_e|_{t=0} e^{[v_i(E_0) - v_a(E_0)]t}, \quad (4)$$

where the absolute value of $v_i - v_a$ is shown in Figure 5 and is also constant in time for $E = E_0$. For $E_0 < E_k$ in a sprite, this condition would produce an exponential relaxation in the rate of optical emissions.

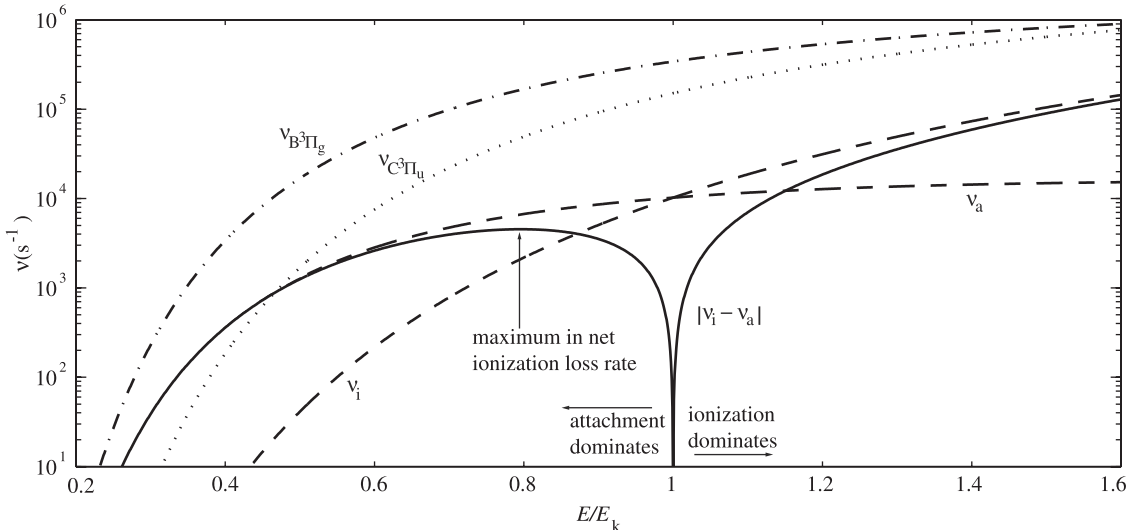


Figure 5. Model ionization and dissociative attachment rates at 70 km altitude. Also shown are the electron impact excitation coefficients v_k for the states $B^3\Pi_g$ and $C^3\Pi_u$ producing optical emissions in the $N_2(1P)$ and $N_2(2P)$ bands, respectively. Each rate shown is proportional to atmospheric density, so values at 60 km are ~ 3.5 times higher than those shown (for 70 km). Data are based on the compilations and calculations of Pasko et al. [1999].

[17] It may be cautioned that a wide variety of physical systems may be well approximated by exponential behavior, sometimes owing to statistical or geometric reasons rather than those relating to local physics. For instance, in the case of elves the temporal structure of optical emissions is locally determined by temporal properties of the causative lightning pulse and at a ground observer site is determined largely by geometrical considerations [Veronis et al., 1999]. These geometrical effects can lead to an apparently closely exponential relaxation of luminosity from the “back” part of elves both in theory and observations for the case of a photometer with a field-of-view as large as that of photometer 11 ($6.6^\circ \times 3.3^\circ$) in the Fly’s Eye.

[18] Nevertheless, the exponential decay feature is found in a majority of the bright sprites observed between 0400 and 0600 UT on 19 July 1998 and often with a more exact fit than the cases shown in Figure 3. Figure 6 shows values of the relaxation time constant τ_o determined via curve fitting to 255 measured photometric pulses exhibiting good to excellent closeness of fit with (1). The photometric recordings were made during 27 sprite sequences which triggered the Fly’s Eye to record ~ 1 s of data from the nine narrow field-of-view, red-filtered photometers and a blue-filtered photometer with a larger field-of-views. The altitudes corresponding to the narrow fields-of-views for these observations were primarily in the range 60–85 km, with considerable uncertainty (± 12 km) based on the possible distance between the sprites and the observer.

[19] The curve fitting is done by finding a least squares fit for periods chosen by hand to correspond well to a decaying exponential form. In some cases the initial period following a bright peak relaxes faster than the exponential fit and not all of it is included. Instead, whenever possible, the fit period is chosen to include many times the duration of τ_o so as to appropriately fix the value of C in (1) to the background luminosity. The quality, or closeness, of fit is then assessed by comparing the values of $\log(y - C)$ from data and fit using the linear correlation parameter R given by Bevington and Robinson [1992, p. 199].

[20] Also shown for reference are some time constants determined with the same algorithm and associated with optical pulses from the same storm but which were determined to be due to elves, based on the criteria described by Barrington-Leigh and Inan [1999]. The apparent close fit in these cases, however, is less significant since the parameter τ_o is barely resolved by the sample period of the photometer. Nevertheless, the values of τ_o given for

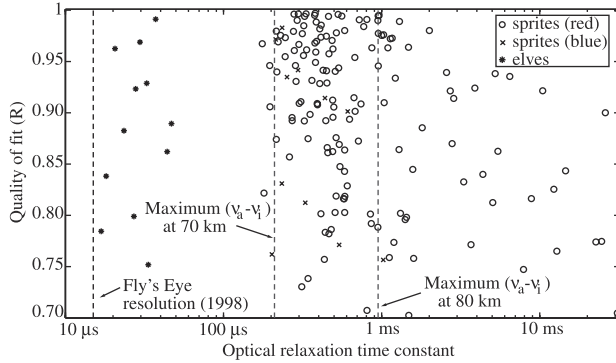


Figure 6. Exponential decay times in sprites. Values shown as crosses and dots are from fits giving $R > 0.7$ using data from one or more red or blue filtered photometers in each of 27 events; each point corresponds to one photometer during one optical pulse of a sprite. The asterisks show the result of fits to photometric signatures of elves.

elves in Figure 6 do give an indication of the timescales for the optical signals due to elves viewed with a narrow field-of-view. The sample period of the data is shown by a dashed vertical line. It is apparent that while the instrument and method are capable of resolving decay constants well below 100 μ s and while the measured variation in τ_o extends over nearly two orders of magnitude for sprites, a lower limit of $\sim 200 \mu$ s exists among the observed sprite cases.

[21] Two more dashed vertical lines show the fastest rate constant $n_e^{-1}(\partial n_e/\partial t) = v_a - v_i$ expected at two different altitudes in the regime where dissociative attachment dominates over ionization. As shown in Figure 5, this maximum rate ($v_a - v_i$)_{max} is reached at $E \simeq 0.8E_k$ and is also the fastest optical relaxation that is predicted for a constant electric field, according to (3). Figure 4 shows the variation of $\tau_a^{\min} = 1/(v_a - v_i)_{\max}$ with altitude. The suggestion that the observed optical relaxation timescale τ_o may be bounded by τ_a^{\min} supports the assumption of an essentially constant electric field during these times.

4. Model and Interpretation

[22] It is remarkable that a constant electric field should arise so repeatably in dynamically driven sprite regions. Below we provide a simple physical explanation of this phenomenon using a large-scale electrodynamic model of sprites [Pasko et al., 1998b] based on the interpretation of current and charge systems in a conducting atmosphere following a lightning discharge, originally proposed by Greifinger and Greifinger [1976]. This discussion will be followed by a consideration of the microscopic time dynamics of optical emissions arising from individual streamer channels constituting sprites, allowing direct comparisons with the observations reported in the preceding section.

4.1. Steady Electric Fields in Sprites

[23] We adopt here a “moving capacitor plate model” of large-scale charge and current systems associated with sprites, as used by Pasko et al. [1998b] and depicted in Figure 7. The model defines a downward moving boundary h_i which separates regions of atmosphere dominated by the conduction (above) and displacement (below) currents. In the case of atmospheric ionization associated with sprites, h_i is closely related to the lower extent of sprite ionization. It is generally believed that the sprite body is highly ionized. The spatially averaged sprite conductivities derived from

ELF measurements are of the order of 10^{-7} mho/m [e.g., Pasko et al., 1998b]. We note that localized conductivity enhancements associated with individual streamer channels are much higher (e.g., $\simeq 5 \times 10^{-5}$ mho/m at 70 km altitude [Pasko et al., 1998a]). The time dynamics of the electric field in this kind of highly conducting medium are defined by the continuity equation $\nabla \cdot \vec{J} = 0$, where \vec{J} is a current flowing through the conductor, which is related to the electric field \vec{E} through Ohms law $\vec{J} = \sigma \vec{E}$. Assuming for simplicity that only the vertical field component is present in sprites and that a sprite has an effective horizontal cross section area S one can rewrite the above continuity equation in the form $\sigma ES = I_{\text{sprite}}$, from which it is clear that the nonzero electric field can persist only if there is a net current flow through the sprite body $I_{\text{sprite}} \neq 0$.

[24] The current I_{sprite} flowing through the sprite body can be readily evaluated using the model depicted in Figure 7. We assume that the system is driven by the lightning current $I(t) = dQ(t)/dt$, which effectively deposits thundercloud charge $Q(t)$ at the altitude h_Q (see Figure 7). The total charge which accumulates at the lower end of the sprite is

$$Q_i(t) = Q(t)h_Q/h_i(t).$$

The current flowing through the sprite is therefore

$$I_{\text{sprite}}(t) = \frac{dQ_i}{dt} = I(t) \frac{h_Q}{h_i(t)} - \frac{Q(t)h_Q}{h_i^2} \frac{dh_i}{dt}. \quad (5)$$

The first term here has to do with the portion of sprite current due to the source (lightning) current, and the second term is due to the descending lower edge of the sprite. The derivative dh_i/dt is generally negative and for estimates can be set to the velocity of positive streamers ($v = 200-2000$ km/s [e.g., Grange et al., 1995; Dhali and Williams, 1987; Babaeva and Naidis, 1997]). Given that the apparent vertical extent of sprites is typically several tens of kilometers (see, for example, Figure 1 and Stanley et al. [1999], Gerken et al. [2000], and Barrington-Leigh et al. [2001]) at this speed streamers can propagate for several milliseconds. As will be illustrated below, during these several milliseconds the electric field remains quasi-constant inside the conducting medium of the sprite, thus supporting the main argument proposed earlier in this paper for the explanation of observed exponential optical relaxation. Substituting specific numbers ($I \simeq 5$ kA, $Q \simeq 100$ C, $h_Q = 10$ km, $h_i \simeq 50$ km) in the above formula indicates that both

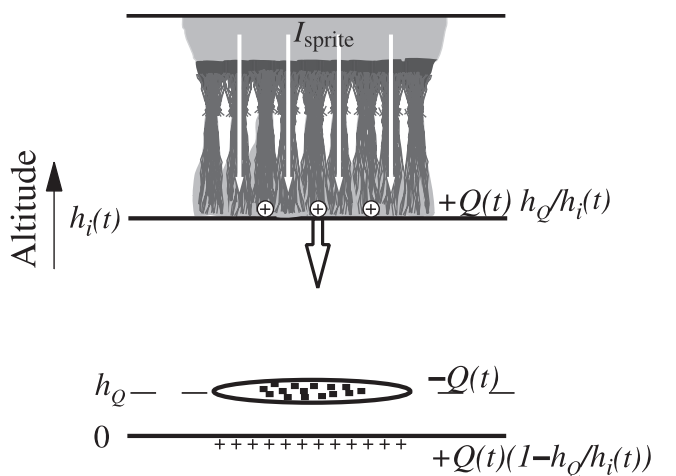


Figure 7. Diagram of charge systems in sprites, after Pasko et al. [1998b].

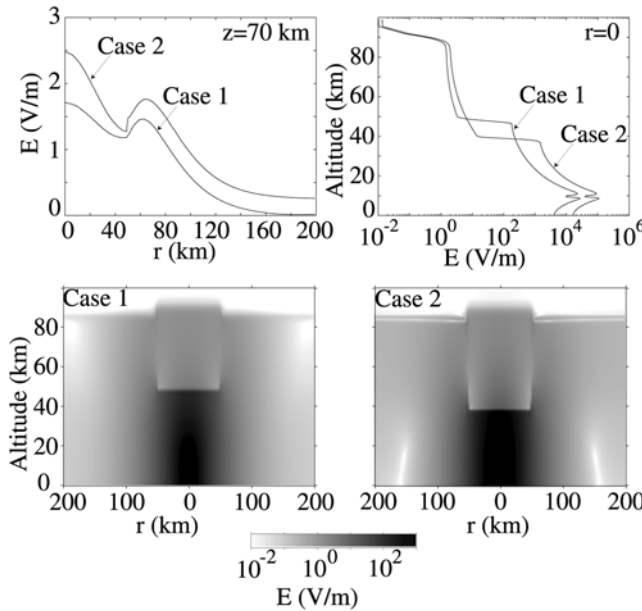


Figure 8. Spatial variation of the model electric field shown at the moment of time 5 ms.

terms can make comparable contributions to the sprite current, which appears to be ~ 1 kA in this case.

[25] Let us now separately consider two cases to illustrate two physical means by which the electric field can be held quasi-constant in the highly conducting medium of a sprite. The first case corresponds to the situation when a steady current continues to flow between cloud and ground and the sprite is static in space, and the second case corresponds to a situation when the source current is zero, but the sprite extends downward with some nonzero velocity.

4.1.1. Case 1. [26] A sprite is modeled as a cylinder with radius $R_s = 50$ km and conductivity $\sigma_s = 10^{-7}$ mho/m as derived from ELF measurements [Pasko et al., 1998b]. The cylinder is assumed to be static, and its lower boundary is placed at $h_i = 50$ km altitude. The ambient ionospheric/conductivity parameters are the same as by Pasko et al. [1998b]. A steady current $I = 5$ kA flows between the cloud (at $h_Q = 10$ km) and the ground, starting at time equal zero and continuing until the end of the simulation (5 ms). This circumstance closely resembles lightning continuing currents associated with sprites recently reported by Cummer and Füllekrug [2001]. Since the sprite is assumed to be static, $h_i = \text{const}$ in (5) and only the first term contributes to the sprite current $I_{\text{sprite}} = \text{const} = Ih_Q/h_i = 1$ kA. We can easily evaluate the static electric field which we expect inside the sprite in this case as $E = I_{\text{sprite}}/(\pi R_s^2 \sigma_s) = 1.3$ V/m. This one-dimensional (1-D) estimate is in excellent agreement with what we observe in our two-dimensional (2-D) numerical experiment for case 1 (see Figures 8 and 9). Figure 8 shows electric fields at the end of the simulation (time = 5 ms), and Figure 9 shows the time dynamics of the electric field at altitude 70 km in the center of the sprite ($r = 0$).

4.1.2. Case 2. [27] In this case we impose an impulse of current lasting ~ 1 ms (rise time 0 s, fall time 0.5 ms, peak current 225 kA), which deposits $Q = 100$ C at $h_Q = 10$ km. Then the charge Q remains constant and the current is zero ($I = 0$) until the end of the simulation. Only the second term in (5) contributes to the sprite current in this case. It is assumed that the sprite lower boundary begins at $h_i(0) = 50$ km and descends at a slowly varying rate. We choose the form $h_i(t) = h_i(0)/[1 + (I_{\text{sprite}}/Qh_Q)h_i(0)t]$, with which the sprite current (in 1-D) defined by the second term in (5) will have exactly the same constant value $I_{\text{sprite}} = 1$ kA as in the previous case 1. In 5 ms the sprite lower boundary extends down to 40 km,

so the effective average sprite velocity is 2000 km/s. The velocity of the sprite in fact is time dependent, being 2500 km/s at $t = 0$ and 1600 km/s at $t = 5$ ms. There are some differences between cases 1 and 2 observed in our numerical experiments (see Figures 8 and 9). These differences are explained by the fact that our two-dimensional numerical model treats the sprite as a conducting cylinder with finite lateral extent and thus contains the horizontal component and the horizontal variation of the electric field (as apparent in Figure 8). This horizontal variation is not present in the simplified one-dimensional analytical model used to derive (5). The 1-D model (5) nevertheless provides a good physical insight and serves for better understanding of more general 2-D simulation results presented in Figures 8 and 9.

[28] These cases illustrate two different means by which the electric field can remain constant in the highly conducting medium of a sprite. Note that the dielectric relaxation constant ε_0/σ_s is 88 μ s inside our model sprite, but the field can stay constant for many milliseconds.

[29] In real sprites the total sprite current $I_{\text{sprite}}(t)$ is effectively carried through the sprite by a number of streamer channels with relatively small cross section [e.g., Gerken et al., 2000]. In order to produce optical emissions, electric fields inside these channels must be of the order of the conventional breakdown threshold field E_k (see Figure 5 and Pasko et al. [1998a]). The above modeling, which assumes that sprites have homogeneous conductivity, certainly is not able to reproduce this aspect of sprites. Nevertheless, the physical reasons for the persistence of electric fields in highly conducting streamer channels constituting real sprites are similar to those described for the two model cases considered above and have to do with either the extension of streamers in space or the temporal growth of the ambient electric field, or a combination of these two effects.

4.2. Time Dynamics of Electron Density and Optical Emissions in Streamer Channels

[30] We now use a simple microscopic model of an individual streamer channel and demonstrate that the exponential optical relaxation is a robust feature of the streamer physics, given that the quasi-steady current is flowing through the streamer channel. In this model the streamer current is assumed to be a given function of time which is dictated by the large-scale electrodynamics of sprites as discussed in section 4.1. The streamer is a physical object which creates large electric field enhancements (an order of magnitude above the conventional breakdown threshold) leading to very high ionization rates around its tip, allowing the streamer to propagate

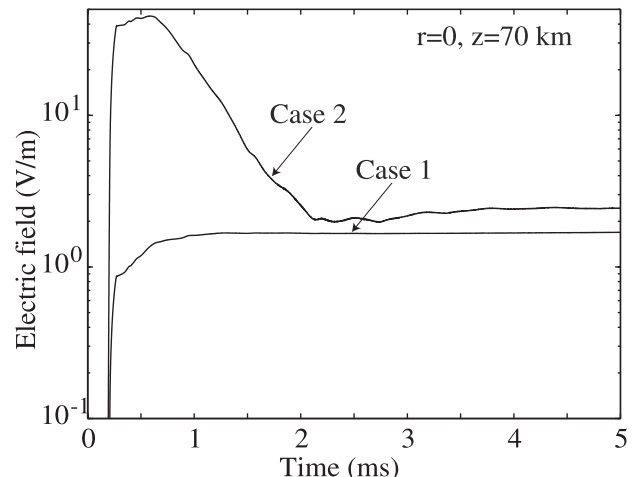


Figure 9. Temporal variation of the model electric field.

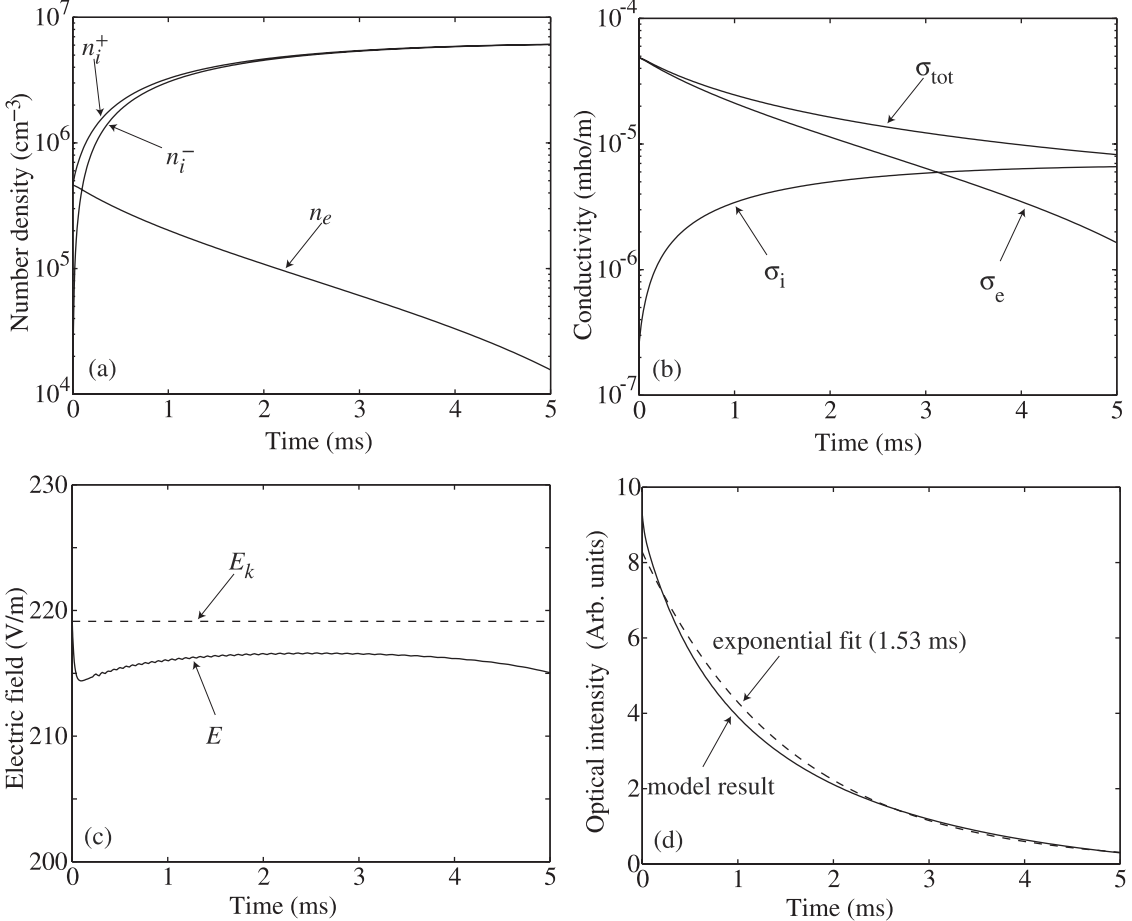


Figure 10. Numerical model of optical relaxation. (a) Electron and ion densities for $\tau_I = 1$ ms, (b) the corresponding conductivities, (c) the corresponding electric field, and (d) resulting optical emissions.

long distances in the form of a filamentary plasma. The physics of streamers has been extensively studied and documented [e.g., Dhali and Williams, 1987; Vitello et al., 1994; Pasko et al., 1998a]. For short streamers (i.e., ~ 1 cm at ground pressure) the electric field value inside the streamer channel behind the streamer tip depends on the applied external field. For streamers which propagate in external fields above the breakdown threshold this value is usually close to the breakdown field (i.e., ~ 30 kV/cm for air at ground pressure) with a general tendency to increase with increased external field [e.g., Dhali and Williams, 1987; Vitello et al., 1994; Babaeva and Naidis, 1997; Kulikovsky, 1997]. Streamers can also propagate in very low external fields, a factor of 6 below the breakdown threshold [Allen and Ghaffar, 1995, and references therein]. In this case the electric field values inside the streamer channel are also very low, of the order of 5 kV/cm at ground pressure [e.g., Grange et al., 1995; Morrow and Lowke, 1997], and are not sufficient to produce any significant optical emissions (see, for example, Figure 5). We assume that bright streamer channels observed in the upper portions of sprites and presumably responsible for the observed optical signatures reported in this paper are produced by strong external electric fields above the conventional breakdown threshold which therefore create large electric fields inside streamer channels.

[31] It is usually assumed that the loss of electrons inside a streamer channel owing to dissociative attachment is not an important process for propagation of short streamers in air (~ 1 cm at ground pressure) [e.g., Babaeva and Naidis, 1997]. The distance 1 cm scales to only $\simeq 40$ m at 60 km altitude in accordance with similarity laws derived by Pasko et al. [1998a]. Assuming that

the streamer propagates with the highest speed measured in sprites, $\sim 10^7$ m/s [Stanley et al., 1999], it would take it ~ 2 ms to travel from 60 to 80 km altitude. The characteristic timescale of dissociative attachment of electrons at 60 km is $\simeq 0.03$ ms and $\simeq 0.1$ ms at 70 km (see Figure 5). Since the timescale of the dissociative attachment process is much smaller than the timescale of propagation of streamers, we expect that dissociative attachment for the long streamers observed in sprites is an important process which is able to affect the streamer internal ionization balance and to control its dynamics. It is expected in particular that the electric field inside the streamer channel stays very close to the conventional breakdown field E_k , at which electron attachment is equalized by ionization (see Figure 5). If the field deviates to lower values, the attachment of electrons is enhanced, reducing the conductivity of the channel. Since the current should be continuous along the streamer channel the conductivity reduction leads to a self-consistent increase in the electric field. If the field deviates to higher values, additional ionization is produced and leads to the enhancement of conductivity; thus the field is self-consistently reduced to maintain continuity of current. The electric field therefore stays at the equilibrium point $E = E_k$. In our modeling below we therefore assume that immediately after the passage of the streamer head we have equal amounts of electrons and positive ions and that $E = E_k$ in the streamer channel. The time duration of our modeling will be limited to several milliseconds, and therefore we account only for the relatively fast processes of electron impact ionization and electron dissociative attachment, ignoring effects of electron and ion recombination and three body attachment processes [e.g., Glukhov et al., 1992, and references therein].

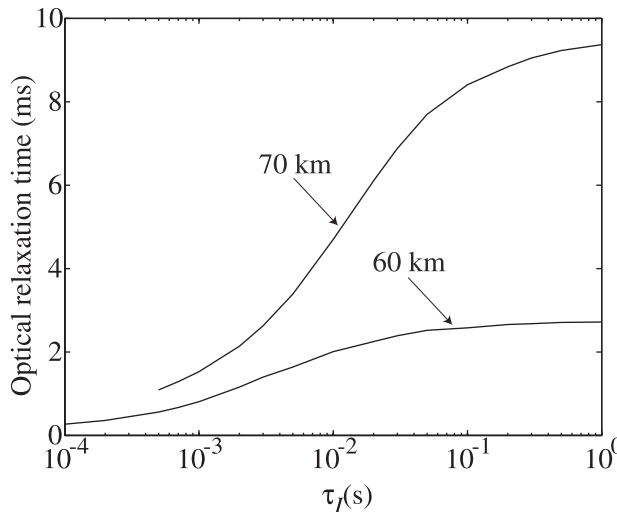


Figure 11. Modeled dependence of τ_o , the optical relaxation time constant, on τ_I , the timescale of change in the sprite current.

[32] We solve the following set of dynamic equations for number densities of electrons n_e , positive n_+ and negative n_- ions:

$$\frac{dn_e}{dt} = [v_i(E) - v_a(E)]n_e \quad (6)$$

$$\frac{dn_+}{dt} = v_i(E)n_e \quad (7)$$

$$n_- = n_+ - n_e. \quad (8)$$

[33] At the initial moment of time $t = 0$, it is assumed that $n_e = n_+ = n_{e,0}$, and $n_- = 0$, where $n_{e,0}$ is the electron number density of stable streamers derived from similarity laws ($n_{e,0} = 5.5 \times 10^6 \text{ cm}^{-3}$ at 60 km and $n_{e,0} = 4.6 \times 10^5 \text{ cm}^{-3}$ at 70 km [Pasko et al., 1998a]). The electric field E in the above equations is assumed to be a function of time determined by current continuity as

$$E = \frac{J(t)}{\sigma} = \frac{J(t)}{en_e\mu_e + e(n_+ + n_-)\mu_i}, \quad (9)$$

where μ_e and μ_i are mobilities of electrons and ions which in the present model are assumed to be constants ($\mu_e = 656 \text{ m}^2/\text{V}\cdot\text{s}$, $\mu_i = 3.4 \text{ m}^2/\text{V}\cdot\text{s}$ at 70 km, and $\mu_e = 189 \text{ m}^2/\text{V}\cdot\text{s}$, $\mu_i = 0.98 \text{ m}^2/\text{V}\cdot\text{s}$ at 60 km [Pasko et al., 1997]). The time-dependent streamer current density $J(t)$ is defined at time $t = 0$ as $J(0) = J_o = (en_{e,0}\mu_e + en_{e,0}\mu_i)E_k$ ($E_k = 761 \text{ V/m}$ and 219 V/m at altitudes 60 and 70 km, respectively) and then assumed to decay as $J(t) = J_o\tau_I/(t + \tau_I)$. The characteristic timescale τ_I of current decay in the sprite is considered as the only input parameter in our model, with all the rest calculated self-consistently. The functional dependence of v_i and v_a on electric field depicted in Figure 5 is used in our calculations.

[34] An interesting aspect of the system which we consider is that even under conditions when $E = E_k$ and n_e is expected to be constant [$v_i(E_k) = v_a(E_k)$], both positive and negative ions accumulate in the streamer body with their densities linearly increasing in time (as is obvious from (7) and (8)). The mobility of ions is only ~ 200 times lower than that of electrons so as soon as the concentrations of ions reach ~ 100 times that of electrons (assuming equal concentrations of negative and positive ions, see further discussion and results presented in Figure 10a) they become the dominant carriers of the current in the streamer.

[35] Before considering the results of numerical calculations let us qualitatively inspect a case when $J(t) = J_o = \text{const}$. The above (9) for the electric field can be rearranged as

$$[en_e\mu_e + e(n_+ + n_-)\mu_i]E = J_o. \quad (10)$$

Even a small increase in ion concentration would lead to an increase in the ion conductivity contribution to J_o and therefore to a drop in the E field. However, even a small reduction in the electric field leads to exponential relaxation of the electron density, which quickly compensates for the increase in the ion conductivity. A remarkable feature of this system is that the electron density relaxes exponentially in time, while the electric field is reduced by a very small amount (specific numbers will be specified below) and essentially remains constant in time with high accuracy.

[36] The current $J(t)$ is not expected to be constant in sprites. In Figure 10 we show results of numerical solutions of the above dynamic system for different τ_I . Figure 10a shows an example of the time dynamics of electrons and ions at 70 km altitude corresponding to a case $\tau_I = 1 \text{ ms}$. The electron dynamics are represented by a straight line on a log-linear plot, thus showing exponential relaxation. Densities of positive and negative ions increase linearly with time and the ion conductivity dominates the total conductivity in the streamer channel after $t \sim 3 \text{ ms}$ (Figure 10b). The maximum variation in the magnitude of the electric field in this case (Figure 10c) does not exceed 2.1%. The electron density exhibits exponential relaxation with timescale 1.53 ms, as does the optical intensity, shown in Figure 10d. Figure 11 provides a summary of all calculated optical relaxation timescales obtained with the model for altitudes 60 and 70 km for τ_I changing between 0.1 ms and 1 s. No changes were observed for $\tau_I > 1 \text{ s}$, which is simply a limiting case of constant $J(t) = J_o$. It is truly remarkable that model relaxation times stay in the range 0.2–10 ms for so wide a range (4 decades) of variation in timescales of sprite current. Our modeling indicates that the electric field tends to stay within several percent of E_k so that optical relaxation does not necessarily proceed at each altitude with the maximum possible rate, which is realized at $E = 0.8E_k$ as shown in Figure 5. We believe that these results provide a simple and straightforward explanation for the experimentally observed exponential optical relaxation in sprites reported in this paper.

5. Discussion

[37] The vertical and possibly horizontal lightning currents evidenced in Figure 3 might each serve as examples of the source $I(t)$ of (5). However, the exponential relaxation observed in sprites is explained here to be a sign of a slowly varying sprite conductivity coupled with any combination of the two terms on the right-hand side of equation (5), relating to either a sustained lightning source term or to the descent of streamers in the sprite.

[38] The exponential relaxation of optical signatures reported here was also observed to be a feature of bright sprites in Fly's Eye data on other days in 1997 and 1998. Determining the degree of ionization in sprites has been a recurring theme and point of debate over the last decade, largely owing to the difficulty of measuring optical output from emission-lines of ionized molecular states. However, on the basis of recent telescopic imaging of sprite fine structure [Gerken et al., 2000] and on the modern understanding of the streamer breakdown process [Pasko et al., 1998a, 2000; Raizer et al., 1998] it seems incontrovertible that intense ionization occurs when filamentary structure is seen in sprites, although this ionization may occur only briefly [e.g., Armstrong et al., 1998a, 2000]. Recently, Barrington-Leigh et al. [2001] showed that with the help of modeling, upwardly concave curvature in sprite halos can be interpreted as a sign of intense ionization augmenting conductivity

gradients and preferentially expelling the electric field. The exponential relaxation of sprite luminosity described in this work also appears to manifest electron density changes, typically over more than 1 order of magnitude.

[39] In addition, the persistence of electric fields near E_k gives reason to predict a characteristic postonset mean electron energy for luminous sprite regions of <3 eV [Pasko et al., 1997, 1999], after possibly more energetic initial processes. This is roughly consistent with spectrally determined time-averaged electron energies of 1–2 eV measured in sprites [Green et al., 1996; Morrill et al., 1998; Green et al., 1998]. In principle, knowledge of the electric field or mean electron energy derived from the exponential relaxation time of optical emissions at a very precisely known altitude could be combined with calibrated photometric intensity to determine the line-integrated absolute electron density in the sprite, by making use of (3) and Figure 5. Such a measurement would, however, require tight constraints on the vertical field of view and on knowledge of the location of the optical source.

6. Summary

[40] Quasi-steady currents in sprites are described in terms of two large-scale physical processes, the slow variation of either the lightning source current or the descent of the sprite's lower edge. In turn, sprite currents which vary slowly compared with the time-scale of electron dissociative attachment to O₂ lead to quasi-constant total conductivity, even while the electron contribution to conductivity is decreasing. This results in a property of streamers driven by strong external electric fields, namely, that the local electric field is maintained self-consistently near the breakdown electric field, E_k .

[41] A quasi-constant electric field just below E_k leads straightforwardly to an exponential relaxation of the electron density and the optical emission rate in sprites. According to our model total ion densities become significant and may dominate the conductivity. Exponential decay of photometric features associated with sprites has been observed in a number of bright sprites and appears to be a form of nonspectroscopic evidence for large ionization changes in sprites. The observed photometric behavior is consistent with the streamer mechanism as the underlying physical process for sprite ionization. In future sprite measurements, more attention could be paid to this phenomenon, in particular in the context of multicolor photometry and photometry with fine altitude discrimination.

[42] **Acknowledgments.** We thank Ken Cummins of Global Atmospheres Inc. for provision of NLDN data, Rick Rairden for the use of an intensified video camera, Langmuir Laboratory for the use of their facilities, Martin Füllekrug for supplying ULF data, and a referee for useful suggestions. This work was supported by the Office of Naval Research under grant N00014-94-1-0100 and by the National Science Foundation under grant NSF-ATM-9731170. Participation of Victor Pasko was supported by the Electrical Engineering department of Pennsylvania State University.

[43] Michel Blanc thanks Richard L. Raider and another referee for their assistance in evaluating this paper.

References

- Allen, N. L., and A. Ghaffar, The conditions required for the propagation of a cathode-directed positive streamer in air, *J. Phys. D Appl. Phys.*, 28, 331, 1995.
- Armstrong, R. A., J. A. Shorter, M. J. Taylor, D. M. Suszynsky, W. A. Lyons, and L. S. Jeong, Photometric measurements in the SPRITES '95 and '96 campaigns of nitrogen second positive (399.8 nm) and first negative (427.8 nm) emissions, *J. Atmos. Sol. Terr. Phys.*, 60, 787–799, 1998a.
- Armstrong, R. A., D. M. Suszynsky, R. Strbley, W. A. Lyons, and T. Nelson, Simultaneous Multi-Color Photometric and Video Recording of SPRITES and their parent lightning mechanisms and energy deposition, *EOS Trans. AGU*, 79(46), Fall Meet. Suppl., F165, 1998b.
- Armstrong, R. A., D. M. Suszynsky, W. A. Lyons, and T. E. Nelson, Multi-color photometric measurements of ionization and energies in sprites, *Geophys. Res. Lett.*, 27, 653–656, 2000.
- Babaeva, N. Y., and G. V. Naidis, Dynamics of positive and negative streamers in air in weak uniform electric fields, *IEEE Trans. Plasma Sci.*, 25, 375, 1997.
- Barrington-Leigh, C. P., and U. S. Inan, Elves triggered by positive and negative lightning discharges, *Geophys. Res. Lett.*, 26, 683–686, 1999.
- Barrington-Leigh, C. P., U. S. Inan, M. Stanley, and S. A. Cummer, Sprites triggered by negative lightning discharges, *Geophys. Res. Lett.*, 26, 3605–3608, 1999.
- Barrington-Leigh, C. P., U. S. Inan, and M. Stanley, Identification of sprites and elves with intensified video and broadband array photometry, *J. Geophys. Res.*, 106, 1741–1750, 2001.
- Bell, T. F., S. C. Reising, and U. S. Inan, Intense continuing currents following positive cloud-to-ground lightning associated with red sprites, *Geophys. Res. Lett.*, 25, 1285–1288, 1998.
- Bevington, P. R., and D. K. Robinson, *Data Reduction and Error Analysis for the Physical Sciences*, 2nd ed., McGraw-Hill, New York, 1992.
- Cummer, S. A., and M. Füllekrug, Unusually intense continuing current in lightning produces delayed mesospheric breakdown, *Geophys. Res. Lett.*, 28, 495–498, 2001.
- Cummer, S. A., and M. Stanley, Submillisecond resolution lightning currents and sprite development: Observations and implications, *Geophys. Res. Lett.*, 26, 3205–3208, 1999.
- Cummer, S. A., U. S. Inan, T. F. Bell, and C. P. Barrington-Leigh, ELF radiation produced by electrical currents in sprites, *Geophys. Res. Lett.*, 25, 1281–1284, 1998.
- Dhali, S., and P. Williams, Two-dimensional studies of streamers in gases, *J. Appl. Phys.*, 62, 4696, 1987.
- Fukunishi, H., Y. Takahashi, M. Kubota, K. Sakanoi, U. S. Inan, and W. A. Lyons, Elves: Lightning-induced transient luminous events in the lower ionosphere, *Geophys. Res. Lett.*, 23, 2157–2160, 1996.
- Gerken, E. A., U. S. Inan, and C. P. Barrington-Leigh, Telescopic imaging of sprites, *Geophys. Res. Lett.*, 27, 2637–2640, 2000.
- Glukhov, V., V. Pasko, and U. Inan, Relaxation of transient lower ionospheric disturbances caused by lightning-whistler-induced electron precipitation bursts, *J. Geophys. Res.*, 97, 16,971–16,979, 1992.
- Grange, F., N. Soulem, J. F. Loiseau, and N. Spyrou, Numerical and experimental determination of ionizing front velocity in a DC point-to-plane corona discharge, *J. Phys. D Appl. Phys.*, 28, 1619, 1995.
- Green, B. D., W. T. Rawlins and M. E. Fraser, Kinetics of excitation of infrared fluorescence by Sprites, *Eos Trans. AGU*, 79(46), Fall Meet. Suppl., F136, 1998.
- Green, B. D., et al., Molecular excitation in sprites, *Geophys. Res. Lett.*, 23, 2161–2164, 1996.
- Greifinger, C., and P. Greifinger, Transient ULF electric and magnetic fields following a lightning discharge, *J. Geophys. Res.*, 81, 2237–2247, 1976.
- Guo, C., and E. Krider, The optical and radiation field signatures produced by lightning return strokes, *J. Geophys. Res.*, 87, 9813–9822, 1982.
- Heavner, M. J., et al., Ionization in sprites, *EOS Trans. AGU*, 79(46), Fall Meet. Suppl., F165, 1998.
- Inan, U. S., C. Barrington-Leigh, S. Hansen, V. S. Glukhov, T. F. Bell, and R. Raider, Rapid lateral expansion of optical luminosity in lightning-induced ionospheric flashes referred to as 'elves', *Geophys. Res. Lett.*, 24, 583–586, 1997.
- Johnson, M., and U. S. Inan, Sferic clusters associated with early/fast VLF events, *Geophys. Res. Lett.*, 27, 1391–1394, 2000.
- Kulikovsky, A. A., The mechanism of positive streamer acceleration and expansion in air in a strong external field, *J. Phys. D Appl. Phys.*, 30, 1515, 1997.
- Lyons, W. A., Sprite observations above the U.S. High Plains in relation to their parent thunderstorm systems, *J. Geophys. Res.*, 101, 29,641–29,652, 1996.
- Morrill, J. S., E. J. Bucsel, V. P. Pasko, S. L. Berg, M. J. Heavner, D. R. Moudry, W. M. Benesch, E. M. Wescott, and D. D. Sentman, Time resolved N₂ triplet state vibrational populations and emissions associated with red sprites, *J. Atmos. Sol. Terr. Phys.*, 60, 811–829, 1998.
- Morrow, R., and J. J. Lowke, Streamer propagation in air, *J. Phys. D Appl. Phys.*, 30, 614, 1997.
- Pasko, V., U. Inan, and T. Bell, Thermal runaway electrons in sprites, paper presented at 1999 URSI National Radio Science Meeting, Boulder, Colo., 1999.
- Pasko, V. P., U. S. Inan, T. F. Bell, and Y. N. Tarantsev, Sprites produced by quasi-electrostatic heating and ionization in the lower ionosphere, *J. Geophys. Res.*, 102, 4529–4561, 1997.
- Pasko, V. P., U. S. Inan, and T. F. Bell, Spatial structure of sprites, *Geophys. Res. Lett.*, 25, 2123–2126, 1998a.
- Pasko, V. P., U. S. Inan, T. F. Bell, and S. C. Reising, Mechanism of ELF radiation from sprites, *Geophys. Res. Lett.*, 25, 3493–3496, 1998b.

- Pasko, V. P., U. S. Inan, and T. F. Bell, Fractal structure of sprites, *Geophys. Res. Lett.*, **27**, 497–500, 2000.
- Rairden, R. L., and S. B. Mende, Time resolved sprite imagery, *Geophys. Res. Lett.*, **22**, 3465–3468, 1995.
- Raizer, Y. P., G. M. Milikh, M. N. Shneider, and S. V. Novakovski, Long streamer in the upper atmosphere above thundercloud, *J. Phys. D Appl. Phys.*, **31**, 3255–3264, 1998.
- Stanley, M., P. Krehbiel, M. Brook, C. Moore, W. Rison, and B. Abrahams, High speed video of initial sprite development, *Geophys. Res. Lett.*, **26**, 3201–3204, 1999.
- Suszczynsky, D. M., R. Roussel-Dupre, W. A. Lyons, and R. A. Armstrong, Blue-light imagery and photometry of sprites, *J. Atmos. Sol. Terr. Phys.*, **60**, 801–809, 1998.
- Thomason, L., and E. Krider, The effects of clouds on the light produced by lightning, *J. Atmos. Sci.*, **39**, 2051–2065, 1982.
- Uman, M., *Lightning Discharge*, Academic, San Diego, Calif., 1987.
- Veronis, G., V. P. Pasko, and U. S. Inan, Characteristics of mesospheric optical emissions produced by lightning discharges, *J. Geophys. Res.*, **104**, 12,645–12,656, 1999.
- Vitello, P. A., B. M. Penetrante, and J. N. Bardsley, Simulation of negative-streamer dynamics in nitrogen, *Phys. Rev. E*, **49**, 5574, 1994.
- Wescott, E. M., H. C. Stenbaek-Nielsen, D. D. Sentman, M. J. Heavner, D. R. Moudry, and F. T. S. Sabbas, Triangulation of sprites, associated halos and their possible relation to causative lightning and micrometeors, *J. Geophys. Res.*, **106**, 10,467–10,477, 2001.
- Winckler, J. R., W. A. Lyons, T. E. Nelson, and R. J. Nemzek, New high-resolution ground-based studies of sprites, *J. Geophys. Res.*, **101**, 6997–7004, 1996.

C. P. Barrington-Leigh, Space Sciences Laboratory, University of California, Berkeley, Berkeley, CA 94720, USA. (cpbl@ssl.berkeley.edu)

V. P. Pasko, Communications and Space Sciences Laboratory, Pennsylvania State University, University Park, PA 16802, USA. (vpasko@psu.edu)

U. S. Inan, Space, Telecommunications, and Radioscience Laboratory, Stanford University, Stanford, CA 94305, USA. (inan@nova.stanford.edu)